WIDE-ANGLE, BROADBAND PLATE POLARIZER WITH 1D PHOTONIC CRYSTAL

S. K. Awasthi

Department of Physics
Amity School of Engineering
Amity University Rajasthan
Jaipur-303002, India

S. P. Ojha

Chaudhary Charan Singh University
Meerut-25004, India

Abstract—Here a photonic crystal plate polarizer (with periodic air gaps), operating over a broad wavelength range extending from 1000 nm to 1770 nm and with a wide angular field of 16° measured in air, is suggested. The polarizer has an average degree of polarization equal to 0.9999, and a high extinction ratio ($> 8.308 \times 10^4$) in transmitted light. Since the plate polarizer does not require optical cements, it is most suitable for use with high power laser systems. It is also smaller in size as compared with multilayered cube polarizers.

1. INTRODUCTION

Photonic crystals (PCs) are artificial multidimensional periodic structures with a period of the order of optical wavelength. These structures can prohibit the propagation of light in specific wavelength ranges. Under appropriate conditions, they can work as filters [1], as omnidirectional reflectors [2–11] or as polarizers [12–17]. A photonic crystal polarizer based on the Brewster angle effect is far more efficient than the well known pile of plates polarizer at Brewster's angle [18], firstly, because absorption losses are almost negligible in PCs [19–23], and secondly, because the general Brewster stack works only at Brewster's angle, whereas the photonic crystal polarizer, by proper designing, can be made to operate quite efficiently over a wide angular range of the incident light.

Polarizers and polarizing beam splitters have found application in many optical systems. Whereas in a polarizer it is only the transmitted or the reflected light that is utilized, in a polarizing beam splitter both the transmitted and the reflected beams are utilized and are of equal significance [16]. Polarizing beam splitters using a one-dimensional photonic crystal have been designed and their performance studied by various researchers [12–17]. It is well known that a high performance polarizing beam splitter is one that operates over a broad spectral region and a wide range of angles of the incident light, the extinction ratio of the desired to the unwanted polarized light in reflection or transmission is large and the transmittance or reflectance for the desired polarization is high [17, 24]. Since it is not possible to fulfill all the above requirements simultaneously in a conventional thin film PBS, a compromise has to be made between them. A polarizer with a large wavelength range usually has a small angular field and vice versa [16].

In this paper, we report a wide-angle, broadband plate polarizer in transmission, which has an average degree of polarization equal to 0.9999, and a high extinction ratio with maximum and minimum limits of 8.189×10^{37} and 8.308×10^{4} respectively in transmitted light, for use with high power laser systems. Wide-angle broadband polarizing beam splitters (PBS) investigated earlier [14–17] are cube polarizers, where multilayers are cemented between two prisms. When these PBS's are used with lasers, the optical cement is dispensed with and bonding is done by means of optical contact [17]. The reason is that optical cements deteriorate as a result of the high power densities frequently encountered with laser beams, and hence the polarizers become useless [16, 25, 26]. The plate polarizer proposed by us is a simple structure with a one-dimensional lattice of air trenches etched in a film of silicon deposited onto a substrate. No optical cementing or optical contacting is required. The polarizer is smaller in size as compared to multilayered cube polarizers, and has a wide angular field of 16° in air, and a wavelength range extending from 1000 nm to 1770 nm.

In Section 2, multilayered thin film polarizers and PBS's which form the background for our study are reviewed. In Section 3, the theoretical analysis upon which our study is based is presented. The mathematical formulation uses a transfer matrix method (TMM) [27, 28]. Section 4 describes the structural design. In Section 5, the performance of the polarizer proposed by us is studied in detail. Finally, conclusions are presented in Section 6.

2. REVIEW OF DEVICES ALREADY INVESTIGATED

MacNeille [14] was the first to design a thin film polarizing beam splitter by cementing multilayers between two prisms. The polarizer worked only at the designed angle of incidence (= 45°). Even a departure of ±2° measured in glass (corresponding to approximately ±3.2° in air) from the design angle caused the performance of the polarizer to deteriorate considerably, especially in reflection. This was because the Brewster angle condition was no longer satisfied. Hence, the MacNeille polarizer could only be used with well collimated light. In addition, the extinction ratio of the polarizer in reflection was low even at the design angle. Mouchart et al. [15] showed that it was possible to increase the angular field of the MacNeille polarizer by optimizing the optical thicknesses of the low and high index materials comprising the multilayer. However, the wavelength range over which the polarizer was effective decreased. Li et al. [16] designed a complicated structure of four material layers arranged periodically on the diagonal face of the MacNeille cube. The optical thicknesses of the layers were chirped to optimize the performance of the polarizer, which was effective over a wider range of wavelengths than the MacNeille and Mouchart's PBS's. For a ±6° variation in the angle of incidence in air he was able to achieve an average degree of polarization of 0.987 in the spectral range 400 to 700 nm. However, extinction ratios achieved were not high enough for some applications. Li et al. [17] next proposed a new high performance thin film PBS that operated at angles greater than the critical angle for total internal reflection. The new PBS, also a cube polarizer, was based on the effects of frustrated total internal reflection (FTIR) and of light interference in thin films, and its performance was several orders of magnitude better than that of the conventional thin film PBS's working at angles below the critical angle. Li [17] also discussed the manufacturing issues, and mentioned the different ways by which the two prisms constituting the cube of the novel PBS could be joined. The first method he suggested was the traditional one of using optical cements. Li's novel PBS required high refractive index substrates and consequently high refractive index optical cements. Optical cements with refractive indices higher than 1.65 are not readily available, so he suggested the use of refractive index matching liquids (which have an upper limit of refractive index ∼ 2.2) instead. But, according to him, these liquids suffered from two defects. Firstly they absorbed some of incident light and secondly they were toxic. He then mentioned another solution to the problem by stating that the two prisms constituting the cube could be optically joined. But according to Dodrowolski [25], obtaining surfaces flat enough for

optical contacting is very difficult on prisms.

3. THEORETICAL ANALYSIS

A three layer periodic thin film structure $n_0|[\mathrm{HLH}]^N|n_0$ is taken, where H and L represent two different material layers with refractive indices n_H (higher) and n_L (lower) respectively, and N is the number of periods of the basic structure [HLH]. The incident and exit media are both air, with refractive index n_0.

The characteristic matrix for an N period structure is given by [27]

$$
\begin{aligned}
[M(d)]^N &= \begin{bmatrix} M_{11}U_{N-1}(a) - U_{N-2}(a) & M_{12}U_{N-1}(a) \\ M_{21}U_{N-1}(a) & M_{22}U_{N-1}(a) - U_{N-2}(a) \end{bmatrix} \\
&\equiv \begin{bmatrix} m_{11} & m_{12} \\ m_{21} & m_{22} \end{bmatrix}
\end{aligned}
\tag{1}
$$

where

$$
\begin{aligned}
M_{11} &= \left(\cos\gamma_1 \cos\gamma_2 \cos\gamma_3 - \frac{p_2}{p_1} \sin\gamma_1 \sin\gamma_2 \cos\gamma_3 \right. \\
&\quad \left. - \frac{p_1}{p_2} \cos\gamma_1 \sin\gamma_2 \sin\gamma_3 - \sin\gamma_1 \cos\gamma_2 \sin\gamma_3 \right), \\
M_{12} &= -i \left(\frac{1}{p_1} \sin\gamma_1 \cos\gamma_2 \cos\gamma_3 + \frac{1}{p_2} \cos\gamma_1 \sin\gamma_2 \cos\gamma_3 \right. \\
&\quad \left. + \frac{1}{p_1} \cos\gamma_1 \cos\gamma_2 \sin\gamma_3 - \frac{p_2}{p_1^2} \sin\gamma_1 \sin\gamma_2 \sin\gamma_3 \right), \\
M_{21} &= -i \left(p_1 \sin\gamma_1 \cos\gamma_2 \cos\gamma_3 + p_2 \cos\gamma_1 \sin\gamma_2 \cos\gamma_3 \right. \\
&\quad \left. + p_1 \cos\gamma_1 \cos\gamma_2 \sin\gamma_3 - \frac{p_1^2}{p_2} \sin\gamma_1 \sin\gamma_2 \sin\gamma_3 \right), \\
M_{22} &= \left(\cos\gamma_1 \cos\gamma_2 \cos\gamma_3 - \frac{p_1}{p_2} \sin\gamma_1 \sin\gamma_2 \cos\gamma_3 \right. \\
&\quad \left. - \frac{p_2}{p_1} \cos\gamma_1 \sin\gamma_2 \sin\gamma_3 - \sin\gamma_1 \cos\gamma_2 \sin\gamma_3 \right).
\end{aligned}
$$

Here $\gamma = \frac{2\pi}{\lambda_0} nd \cos\theta$, θ is the ray angle inside the layer of refractive index n, and thickness d and is related to the angle of incidence θ_0 by

$$
\cos\theta = \left[1 - \frac{n_0^2 \sin^2\theta_0}{n^2} \right]^{1/2}
\tag{2}
$$

λ_0 is the free space wavelength.

The subscripts 1, 2 and 3 refer to the layers HLH respectively.

For s-polarization

$$p = n \cos \theta \tag{3}$$

For p-polarization

$$p = \frac{\cos \theta}{n} \tag{4}$$

U_N are the Chebyshev polynomials of the second kind

$$U_N(a) = \frac{\sin \left[(N + 1) \cos^{-1} a \right]}{[1 - a^2]^{1/2}} \tag{5}$$

where

$$a = \frac{1}{2} [M_{11} + M_{22}], \tag{6}$$

The reflection and transmission coefficients of the N period structure are given by

$$r = \frac{R'}{A'} = \frac{(m_{11} + m_{12}p_0) p_0 - (m_{21} + m_{22}p_0)}{(m_{11} + m_{12}p_0) p_0 + (m_{21} + m_{22}p_0)} \tag{7}$$

$$t = \frac{T'}{A'} = \frac{2p_0}{(m_{11} + m_{12}p_0) p_0 + (m_{21} + m_{22}p_0)} \tag{8}$$

where for s-polarization

$$p_0 = n_0 \cos \theta_0 \tag{9}$$

and for p-polarization

$$p_0 = \frac{\cos \theta_0}{n_0} \tag{10}$$

A', R' and T' are the amplitudes of the electric vectors of the incident, reflected and transmitted waves respectively.

The reflectivity and transmissivity are

$$\Re = |r|^2 \tag{11}$$

$$\mathrm{T} = |t|^2 \tag{12}$$

4. STRUCTURAL DESIGN

The high and low index layers shown in Fig. 1 have been taken to be those of silicon and air respectively. Silicon has been chosen because it is transparent in the region of investigation, has a high index of refraction in this region ($n_H = 3.6$), and a high laser damage threshold. Also, highly developed nano fabrication techniques exist for silicon on account of its use in integrated circuits [29]. To minimize losses, the low index layer has been taken to be that of air ($n_L = 1.0$). Thus, a high index ratio ($n_H/n_L = 3.6$) is achieved giving a large wavelength range of maximum reflectivity for s-polarized light.
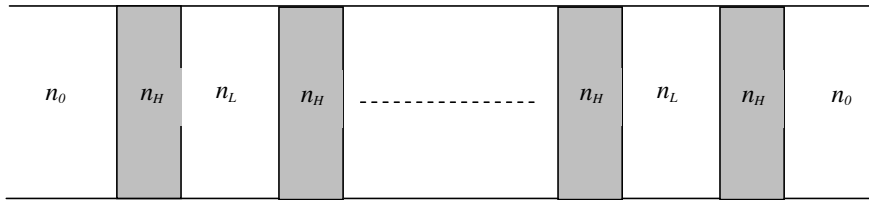

Figure 1. Depiction of a one-dimensional **HLH** periodic lattice.

The proposed structure can be fabricated by deep reactive ion etching (DRIE) in a film of silicon deposited onto a substrate. Thus, air trenches are formed at periodic intervals throughout the entire silicon film (Fig. 2). Such a structure may resemble the one described earlier in Reference [30], where a one-dimensional lattice of air trenches of width 45 nm was fabricated by electron beam lithography and deep reactive ion etching (DRIE) through an AlGaAs surface waveguide structure. Advanced silicon etching techniques based on DRIE to fabricate Si-air periodic structures for photonic applications have been discussed in Reference [31]. Deep reactive ion etching is a dry etch micromachining method. The use of ICP (inductively coupled plasma) allows for extremely high silicon etch rates using standard Cryo and Bosch processes. The capabilities of modern DRIE'S are high aspect ratios (upto 50:1), deep etching (10 μm–700 μm) and high etch rate (4–20 μm/min.) [32].

In our case, the size of the laser beam would need to be less than the 0.7 mm dimension of the silicon-air structure in order to avoid edge effects. This may be straightforwardly achieved by using, say, a cylindrical lens.
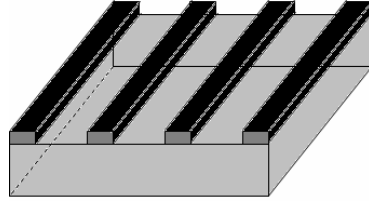
Figure 2. Structural design of polarizer.

5. RESULTS AND DISCUSSION

The Brewster angle condition for the structure is

$$\sin\theta_0 = \frac{n_H}{\sqrt{1 + n_H^2}} \tag{13}$$

When this condition is fulfilled, the s-polarized light will be reflected and the p-polarized light will be transmitted. For the materials selected, (silicon and air), condition (13) will be fulfilled at Brewster angle $74°27'$. The lattice period (Λ) is taken to be equal to $435\,\text{nm}$. For each choice of n_H and n_L, there is a particular value of the filling fraction ($= d_L/\Lambda$) which gives maximum angular field of the polarizer. d_L is the thickness of the air gap. The optimum filling fraction $\eta_{\text{opt.}}$ corresponding to maximum angular field was numerically computed to be equal to 0.84, corresponding to which d_L was calculated to be equal to $365.4\,\text{nm}$. The silicon layers on either side of the air gap in one period of the ternary structure were taken to be equal to each other ($= 34.8\,\text{nm}$). The number of periods N, of the structure was optimized to give maximum reflectivity of the s-polarized component, and also to reduce the ripples in the curve of reflectivity of s-polarized wave versus wavelength (Fig. 3(b)) for the range of angles studied. N_{opt} was numerically computed to be equal to 21.

Using expressions (1)–(12) the reflectivity and transmissivity spectra for the s and p polarized waves were plotted for angles of incidence equal to $64°$, $69°$, $74°27'$ and $80°$ (Fig. 3 and Fig. 4). For the range of angles considered, the transmissivity of the s-polarized wave has a maximum value of 1.1×10^{-5} and a minimum value of 9.4×10^{-38} while that of the p-polarized wave varies between a minimum of 0.8465 and a maximum of 1. In transmission, the degree of polarization is defined by [16]

$$P_T = \left| \frac{T_P - T_S}{T_P + T_S} \right| \tag{14}$$
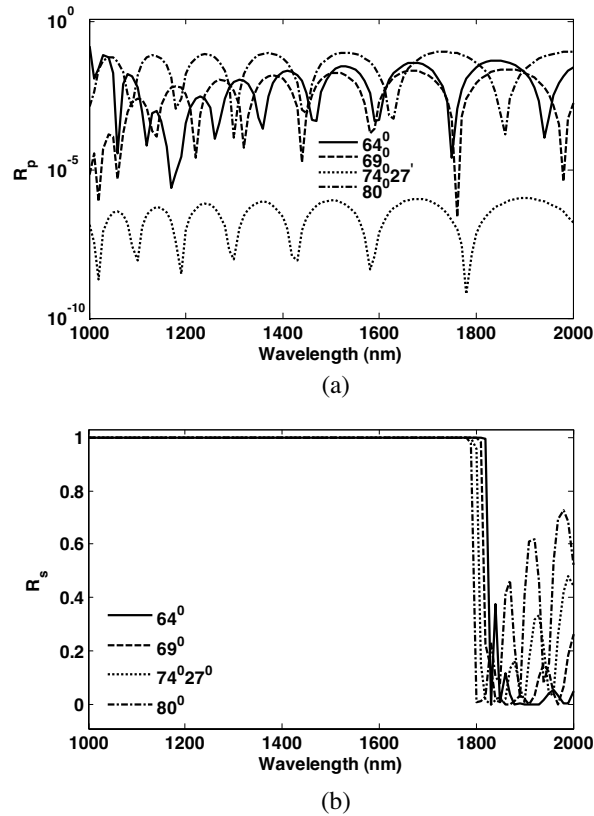
Figure 3. (a) Calculated reflectivity spectra of Si/Air/Si 21 period structure ($\Lambda = 435$ nm) for p-polarized light at different angles of incidence (64°-Sol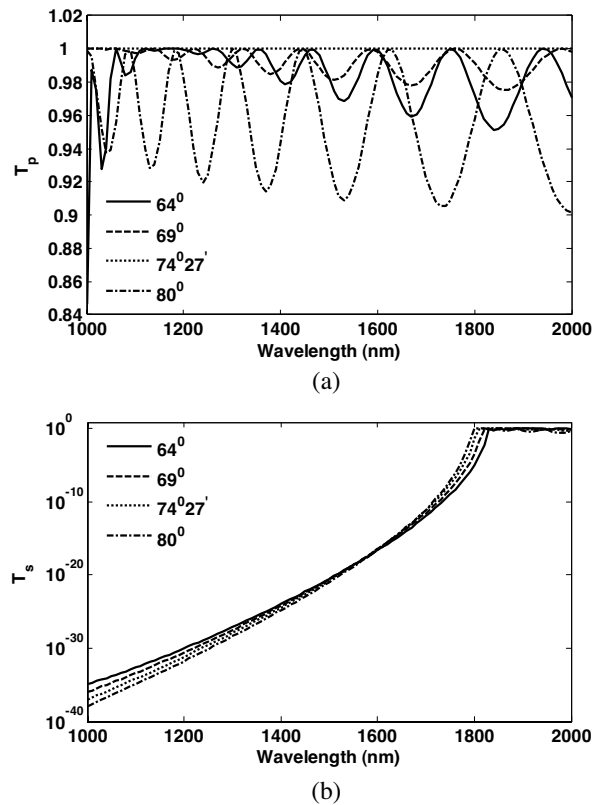id line, 69°-dashed line, 74°27′-dotted line, 80°-dash-dotted line), (b) Calculated reflectivity spectra of Si/Air/Si 21 period structure ($\Lambda = 435$ nm) for s-polarized light at different angles of incidence (64°-Solid line, 69°-dashed line, 74°27′-dotted line, 80°-dash-dotted line).

where T_P, T_S are the transmittances for p- and s-polarized light respectively. The average value of P_T for the range of wavelengths and angles investigated was calculated to be 0.9999. The high value of P_T obtained may be attributed to the fact that the transmissivity of the s-polarized wave (T_S) is extremely low, with a maximum value of only 1.1×10^{-5}.

The extinction ratio in transmission, defined by

$$(E.R.)_T = \frac{T_P}{T_S}$$

varies between a minimum of 8.308×10^4 and a maximum of 8.189×10^{37} (Fig. 6(a)). The angular field of the device for transmitted light is $16°$ in air, and the effective wavelength range is $1000\,\text{nm}$–$1770\,\text{nm}$.

Analysis of the reflected light shows that the reflectivity of the

Figure 4. (a) Calculated transmission spectra of Si/Air/Si 21 period structure ($\Lambda = 435\,\text{nm}$) for p-polarized light at different angles of incidence ($64°$-Solid line, $69°$-dashed line, $74°27'$-dotted line, $80°$-dash-dotted line), (b) Calculated transmission spectra of Si/Air/Si 21 period structure ($\Lambda = 435\,\text{nm}$) for s-polarized light at different angles of incidence ($64°$-Solid line, $69°$-dashed line, $74°27'$-dotted line, $80°$-dash-dotted line).
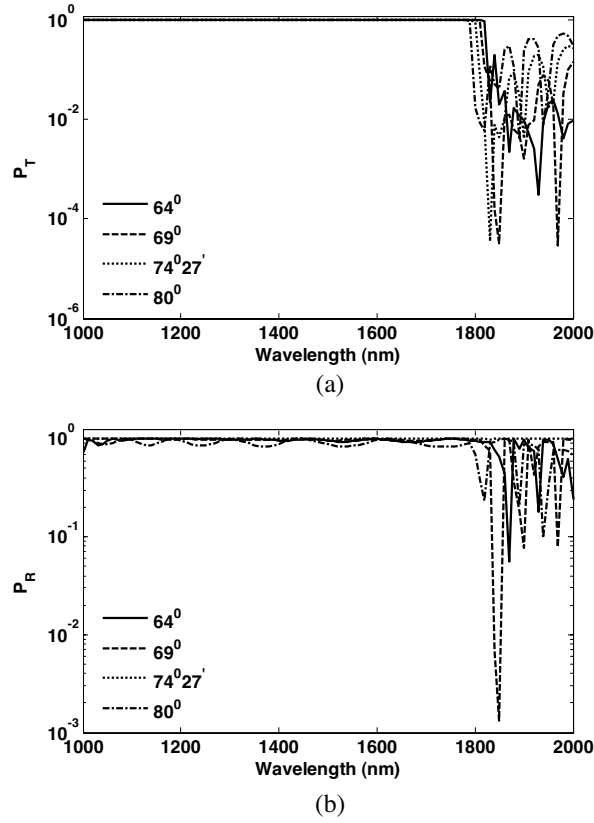
(a)

(b)

Figure 5. (a) Calculated degree of polarization (P_T) of Si/Air/Si 21 period structure ($\Lambda = 435\,\text{nm}$) in transmission at different angles of incidence (64°-Solid line, 69°-dashed line, 74°27′-dotted line, 80°-dash-dotted line), (b) Calculated degree of polarization (P_R) of Si/Air/Si 21 period structure ($\Lambda = 435\,\text{nm}$) in reflection at different angles of incidence (64°-Solid line, 69°-dashed line, 74°27′-dotted line, 80°-dash-dotted line).

s-polarized light is ~ 1.0 in the wavelength range $1000\,\text{nm}$–$1770\,\text{nm}$, while that of the p-polarized component varies between a minimum of 6.0×10^{-7} and a maximum of 0.1535. In reflection, the degree of polarization is defined by [16]
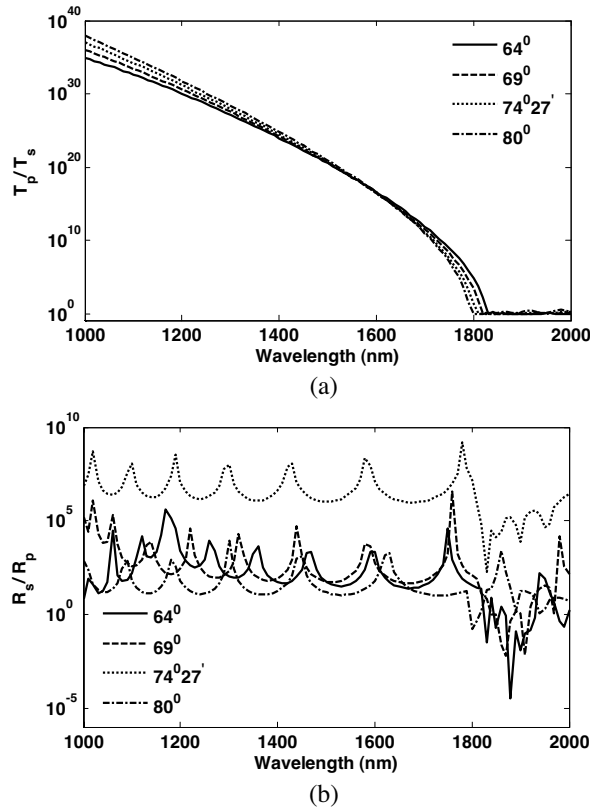
$$P_R = \left| \frac{R_P - R_S}{R_P + R_S} \right|$$

Figure 6. (a) Calculated extinction ratio $(E.R.)_T$ of Si/Air/Si 21 period structure ($\Lambda = 435\,\text{nm}$) in transmission at different angles of incidence (64°-Solid line, 69°-dashed line, 74°27′-dotted line, 80°-dash-dotted line), (b) Calculated extinction ratio $(E.R.)_R$ of Si/Air/Si 21 period structure ($\Lambda = 435\,\text{nm}$) in reflection at different angles of incidence (64°-Solid line, 69°-dashed line, 74°27′-dotted line, 80°-dash-dotted line).

where R_P and R_S are the reflectances for p- and s-polarized light respectively. The average value of P_R was calculated to be 0.9276.

The extinction ratio in reflection, defined by

$$(E.R.)_R = \frac{R_S}{R_P}$$

varies between a minimum of 6.514 and a maximum of 4.943×10^8 (Fig. 6(b)).

Figures 5(a) and 5(b) are plots of the degree of polarization (P_T, P_R) versus wavelength for angles of incidence $64°$, $69°$, $74°27'$ and $80°$. Comparison of the results obtained for reflected light with the corresponding ones obtained for transmitted light reveal that the performance of the polarizer is better in transmission.

Above analysis shows that the device proposed by us is a more efficient polarizer than a polarizing beam splitter. To the best of our knowledge, a wide angle broadband plate polarizer, which has a high extinction ratio in transmission, with minimum and maximum limits of 8.308×10^4 and 8.189×10^{37} respectively has not been reported before.

6. CONCLUSION

A wide angle broadband plate polarizer with an angular field of $16°$ measured in air and operating over a wavelength range extending from $1000 \, \text{nm}$ to $1770 \, \text{nm}$ is proposed. The polarizer is a simple structure with a one-dimensional lattice of air trenches etched in a film of silicon deposited onto a substrate. It has a high performance in transmission, with an average degree of polarization equal to 0.9999, and extinction ratio varying between a minimum of 8.308×10^4 and a maximum of 8.189×10^{37} in transmitted light. As no optical cements are used, the polarizer is suitable for use with high power laser systems. It is also smaller in size as compared with multilayered cube polarizers.

ACKNOWLEDGMENT

REFERENCES

1. Choudhury, P. K., P. Khastgir, S. P. Ojha, D. K. Mahapatra, and O. N. Singh, "Design of an optical filter as a monochromatic selector from atomic emissions," *J. Opt. Soc. Am. A*, Vol. 9, 1007–1010, 1992.

2. Fink, Y., J. N. Winn, S. Fan, C. Chen, J. Michel, J. D. Joannopoulos, and E. L. Thomas, "A dielectric omnidirectional reflector," *Science*, Vol. 282, 1679–1682, 1998.

3. Zandi, O., Z. Atlasbaf, and K. Forooraghi, "Flat multilayer dielectric reflector antennas," *Progress In Electromagnetics Research*, PIER 72, 1–19, 2007.

4. Aissaoui, M., J. Zaghdoudi, M. Kanzari, and B. Rezig, "Optical properties of the quasi-periodic one-dimensional generalized multilayer Fibonacci structures," *Progress In Electromagnetics Research*, PIER 59, 69–83, 2006.

5. Maka, T., D. N. Chigrin, S. G. Romanov, and C. M. S. Torres, "Three dimensional photonic crystals in the visible regime," *Progress In Electromagnetics Research*, PIER 41, 307–335, 2003.

6. Wu, C.-J., "Transmission and reflection in a periodic superconductor/dielectric film multilayer structure," *Journal of Electromagnetic Waves and Applications*, Vol. 19, 1991–1996, 2005.

7. Zhao, L. P., X. Zhai, B. Wu, T. Su, W. Xue, and C.-H. Liang, "Novel design of dual-mode bandpass filter using rectangle structure," *Progress In Electromagnetics Research B*, Vol. 3, 131–141, 2008.

8. Rojas, J. A. M., J. Alpuente, J. PiËœeneiro, and R. Sanchez, "Rigorous full vectorial analysis of electromagnetic wave propagation in 1D," *Progress In Electromagnetics Research*, PIER 63, 89–105, 2006.

9. Zheng, Q. R., Y. Q. Fu, and N. C. Yuan, "Characteristics of planar PBG structures with a cover layer," *Journal of Electromagnetic Waves and Applications*, Vol. 20, No. 11, 1439–1453, 2006.

10. Chigrin, D. N., A. V. Lavrinenko, D. A. Yarotsky, and S. V. Gaponenko, "Observation of total omnidirectional reflection from a one-dimensional-dielectric lattice," *Appl. Phys. A*, Vol. 68, 25–28, 1999.

11. Deopura, M., C. K. Ullal, B. Temelkuran, and Y. Fink, "Dielectric omnidirectional-visible reflector," *Opt. Lett.*, Vol. 26, 1197–1199, 2001.

12. Thomsen, M. and Z. L. Wu, "Polarizing and reflective coatings based on half-wave layer pairs," *Appl. Opt.*, Vol. 36, 307–313, 1997.

13. Monga, J. C., "Multilayer thin-film polarizers with reduced electric-field intensity," *J. Mod. Opt.*, Vol. 36, 769–784, 1989.

14. MacNeille, S. M., "Beam splitter," U. S. patent 2, 403, 731, July 9, 1946.

15. Mouchart, J., J. Begel, and E. Duda, "Modified MacNeille cube

polarizer for a wide angular field," *Appl. Opt.*, Vol. 28, 2847–2853, 1989.

16. Li, L. and J. A. Dobrowolski, "Visible broadband, wide-angle, thin-film multilayer polarizing beam splitter," *Appl. Opt.*, Vol. 35, 2221–2225, 1996.

17. Li, L. and J. A. Dobrowolski, "High-performance thin-film polarizing beam splitter operating at angles greater than the critical angle," *Appl. Opt.*, Vol. 39, 2754–2771, 2000.

18. Hecht, E., *Optics*, 4th edition, 349, Addison Wesley, 2002.

19. Li, B., K.-J. Lee, H.-T. Chou, and W. Gu, "A polarization compensation approach utilizing a paraboloid photonic-crystal structure for crossed-dipole excited reflector antennas," *Progress In Electromagnetics Research*, PIER 85, 393–408, 2008.

20. Srivastava, S. K. and S. P. Ojha, "Photonic band gaps in one-dimensional metallic star waveguide structure," *Progress In Electromagnetics Research*, PIER 84, 349–362, 2008.

21. Si, L.-M. and X. Lv, "CPW-FED multi-band omni-directional planar microstrip antenna using composite metamaterial resonators for wireless communications," *Progress In Electromagnetics Research*, PIER 83, 133–146, 2008.

22. Srivastava, R., K. B. Thapa, S. Pati, and S. P. Ojha, "Design of photonic band gap filter," *Progress In Electromagnetics Research*, PIER 81, 225–235, 2008.

23. Dubey, R. S. and D. K. Gautam, "Development of simulation tools to study optical properties of one-dimensional photonic crystals," *Journal of Electromagnetic Waves and Applications*, Vol. 22, No. 5–6, 849–860, 2008.

24. Li, L., "The design of optical thin film coatings with total and frustrated total internal reflection," *Optics and Photonics News*, 24–30, 2003.

25. Dobrowolski, J. A. and A. Waldorf, "High-performance thin film polarizer for the UV and visible spectral regions," *Appl. Opt.*, Vol. 20, 111–116, 1981.

26. Gilo, M. and K. Rabinovitch, "Design parameters of thin-film cubic-type polarizers for high power lasers," *Appl. Opt.*, Vol. 26, 2518–2521, 1987.

27. Born, M. and E. Wolf, "Basic properties of the electromagnetic field," *Principles of Optics*, 1–70, Cambridge University Press, U. K., 1980.

28. Yeh, P., "Optics of periodic layered media," *Optical Waves in Layered Media*, 118–142, Wiley, New York, 1998.

29. Cowan, B., "Optical damage threshold of silicon for ultrafast infrared pulses," *Proceedings of AIP Conference on Advanced Accelerator Concepts*, Vol. 877, 837–843, 2006.

30. Bristow, A. D., V. N. Astratov, R. Shimada, I. S. Culshaw, M. S. Skolnick, D. M. Whittaker, A. Tahraoui, and T. F. Krauss, "Polarization conversion in the reflectivity properties of photonic crystal waveguides," *IEEE J. Q. E.*, Vol. 38, 880–884, 2002.

31. Marty, F., L. Rousseau, B. Saadany, B. Mercier, O. Français, Y. Mita, and T. Bourouina, "Advanced silicon etching techniques based on deep reactive ion etching (DRIE) for silicon harms and 3D micro- and nano-structures," *Microelectronics Journal, Elsevier Science*, Vol. 36, 673–677, 2005.

32. Jeff Raaphorst, Process Engineer, Micralyne Inc., "DRIE-Deep Reactive Ion Etching," http://www.micralyne.com/edition4.new-slyne/html.